Sonoluminescence

Matt Knight
100324662

02/24/10

Abstract:

The effect of water preparation on sonoluminescence was studied. Single and multiple bubble sonoluminescence was observed within a narrow range of conditions. Water temperature and dissolved gas content were found to be most significant to the formation of sonoluminescent bubbles.

Theory:

Sonoluminescence (SL) occurs when a bubble, driven by ultrasound, collapses to a very small radius. This phenomenon can occur in a resonant cavity, with a trapped bubble as is the case in Single Bubble Sonoluminescence (SBSL), or with a large driving amplitude and free floating or cavitation bubbles as observed in Multiple Bubble Sonoluminescence (MBSL).

Resonance in a cell occurs at the frequency given by the equation below.

$$f_{n_x n_y n_z} = \frac{c}{2\pi} \sqrt{\left(\left(\frac{n_x \pi}{L_x} \right)^2 + \left(\frac{n_y \pi}{L_y} \right)^2 + \left(\frac{n_z \pi}{L_z} \right)^2 \right)}$$

Where n is the mode, c is the speed of sound in water, and L is the dimension. For the purpose of this experiment we are studying the 1, 1, 3 mode of resonance, in which the three pressure nodes are located along the centerline of the cell, spaced equidistant. The expected resonant frequency in this case, at 10 C is:

$$f_{1,1,3} \cong 28.811 kHz$$

There are two currently accepted models for the mechanism behind SL, adiabatic collapse with a shockwave, and microjet collapse. In the case of both models, the bubble is driven by the ultrasound to expand to a radius of approximately 50 microns during the rarefaction of the sound wave, then driven to collapse to a radius of approximately 0.5 microns during compression. Following the compression cycle, the bubble rebounds several times, as shown in figure 1, below, from Putterman 1995.[1]

---

[1] Putterman 1995

Figure 1: Collapse and rebound of trapped bubble, from Putterman 1995.
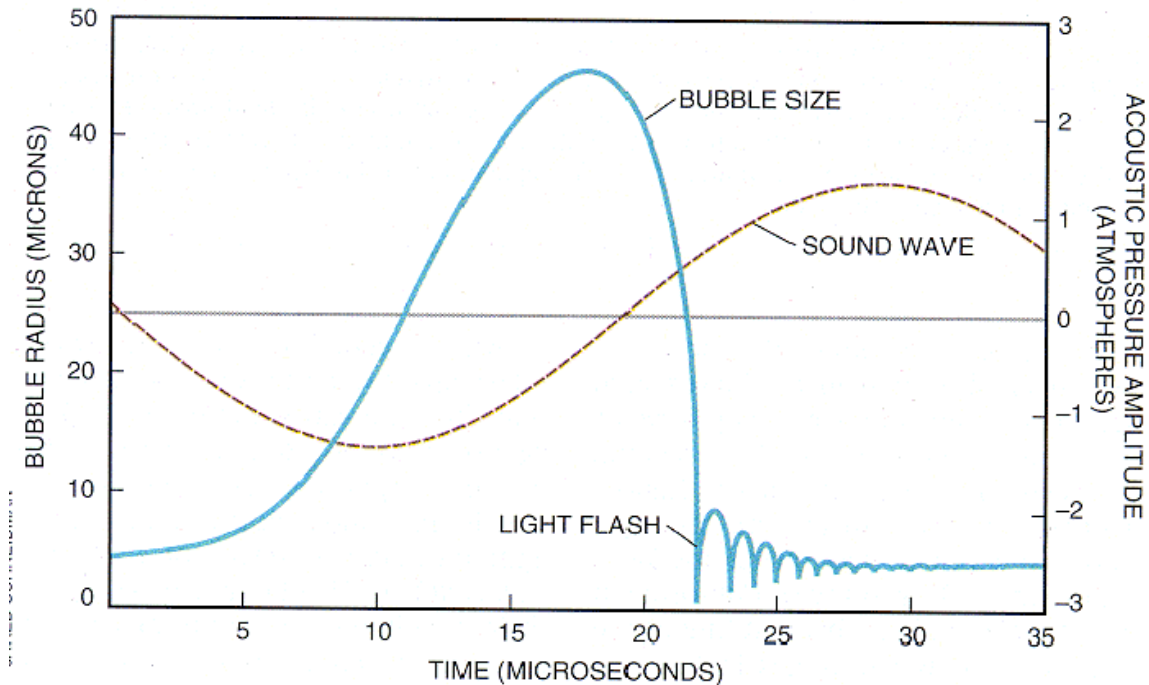
In the adiabatic compression model, a shockwave is formed within the bubble. This shockwave precedes the collapsing bubble wall during the compression of the bubble. As the bubble collapses to 0.5 microns, the shockwave collapses to almost 0 radius. The collapsing shockwave superheats the gas within the bubble, forming light emitting plasma.[2] This process is highly dependent on the symmetry of the bubble; any asymmetries during the collapse of the bubble will lead to an increase in radius of the shockwave. As the heating is dependent on a small radius, this would result in a much lower temperature and no light emitted.

In the microjet collapse model, the bubble collapses asymmetrically, forming a microjet along the surface of the wall. This microjet travels across the bubble as supersonic speed, impacting the opposing wall. On impact, the bubble wall fractures. The energy released by this fracture ionizes the gas within bubble and light is emitted. Microjet collapse does not depend on the symmetry of the bubble, as the jet itself is an asymmetric feature. Formation of microjets has been noted in the collapse of cavitation bubbles, as shown in figure 2 below.

---

[2] Gutenkunst 2002

Figure 2: Microjet formation in microgravity, from the European Space Agency.[3]

(b)
Cavitation bubble

292 µs

Cavitation bubble achieves maximal radius.

(c)

584 µs

Cavitation bubble collapses.

(d)
Microjet

1000 µs

Microjet propagates to the right.
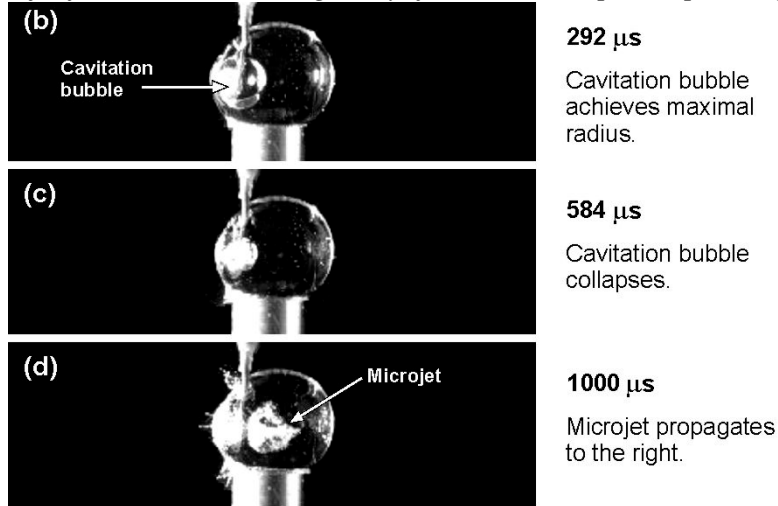
Apparatus:

1. Signal Generator
2. Sonoluminescence apparatus (amplifier/filter/power supply)
3. Ultrasound horn
4. Resonant cell – plastic, 5.4 cm x 5.4 cm x 12 cm, piezoelectric transducer secured to bottom of cell.
5. Oscilloscope
6. Digital Camera
7. Thermocouple and multimeter

The setup used in this experiment is shown in figure 3 below.

---

[3] ESA: Team Flash and Splash - http://www.flashandsplash.ch/Project/negative.JPG

Figure 3: Experimental setup showing signal generator, amplifier, oscilloscope, ultrasound horn and cell.
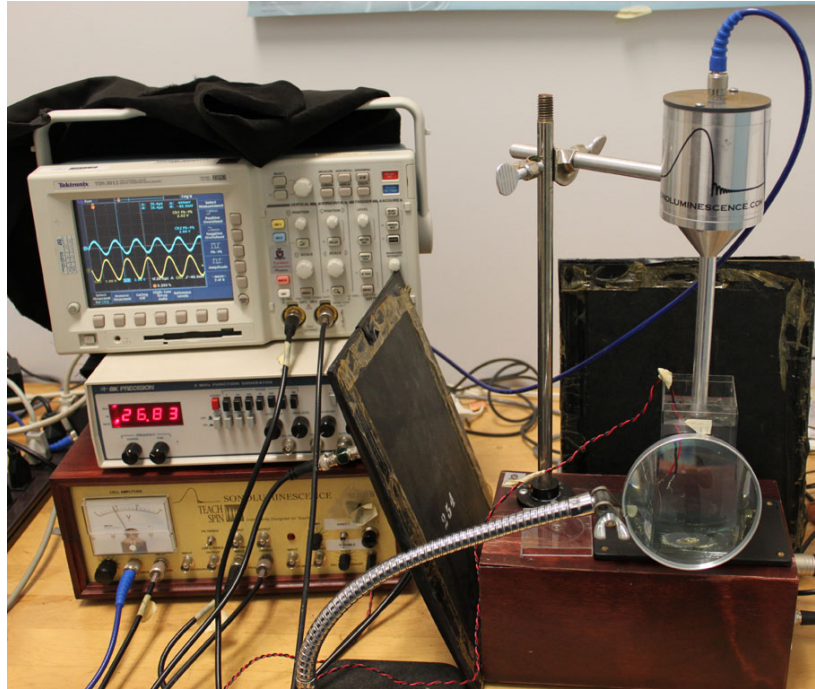
Procedure:

First, cold distilled water was degassed by subjecting it to a vacuum. Once the dissolved gas concentration was suitably reduced, the cell was filled to a depth of 10 cm. The ultrasound horn was immersed in the cell, so that the end of the horn was submerged to a depth of 0.5 cm. A filament was placed in the cell as well, to generate bubbles as necessary.

The signal generator was used to send a sine wave through the sonoluminescence apparatus, which served to amplify the signal. The resonance frequency was determined by adjusting the input frequency on the signal generator, and measuring the output amplitude from the transducer mounted in the cell. This data was used to plot the quality curves shown in the results.

Once the resonance frequency was determined, the filament was used to generate bubbles and the amplification was adjusted to trap bubbles at the pressure nodes in the resonant cell. The amplitude of the input signal was then adjusted until sonoluminescence was observed.

During the course of the experiment, the water in the cell would warm. As a result of this, the temperature of the water was checked periodically with the thermocouple. The thermocouple was placed at the bottom corner of the cell.

Results:

Initial distilled water samples resulted in significant clipping occurring in the ultrasound signal. The signal was most affected at the approximate frequency of the resonance peak, between 26.34 kHz and 26.68 kHz, as shown in figure 4 below.

Figure 4: Quality Curve for 17 degree distilled water, showing drop in output amplitude at resonant frequency.
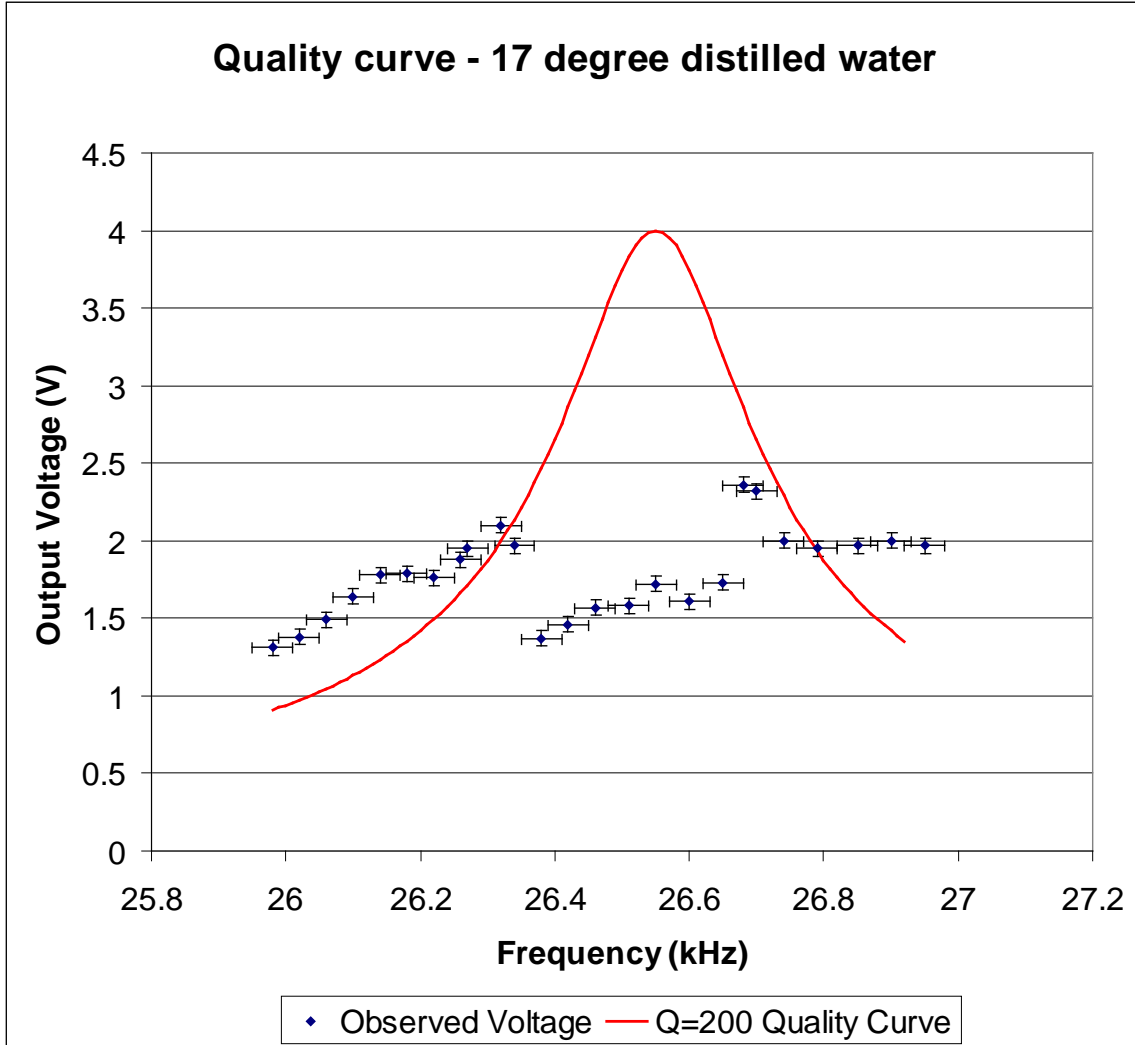
Also shown in the above figure is the Q=200 Quality curve calculated using the universal resonance curve model.[4]

---

[4] Universal Resonance Curve: http://www.art-sci.udel.edu/ghw/phys245/05S/classpages/resonance-linear.html

Subsequent water samples showed improved response, resulting in much better quality curves, as well as better signal quality observed in the resonant signal. Figures 5, 6, 7, and 8 show the quality curves obtained.

Figure 5: Quality Curve for 8 degree distilled water after 15 minutes degassing.
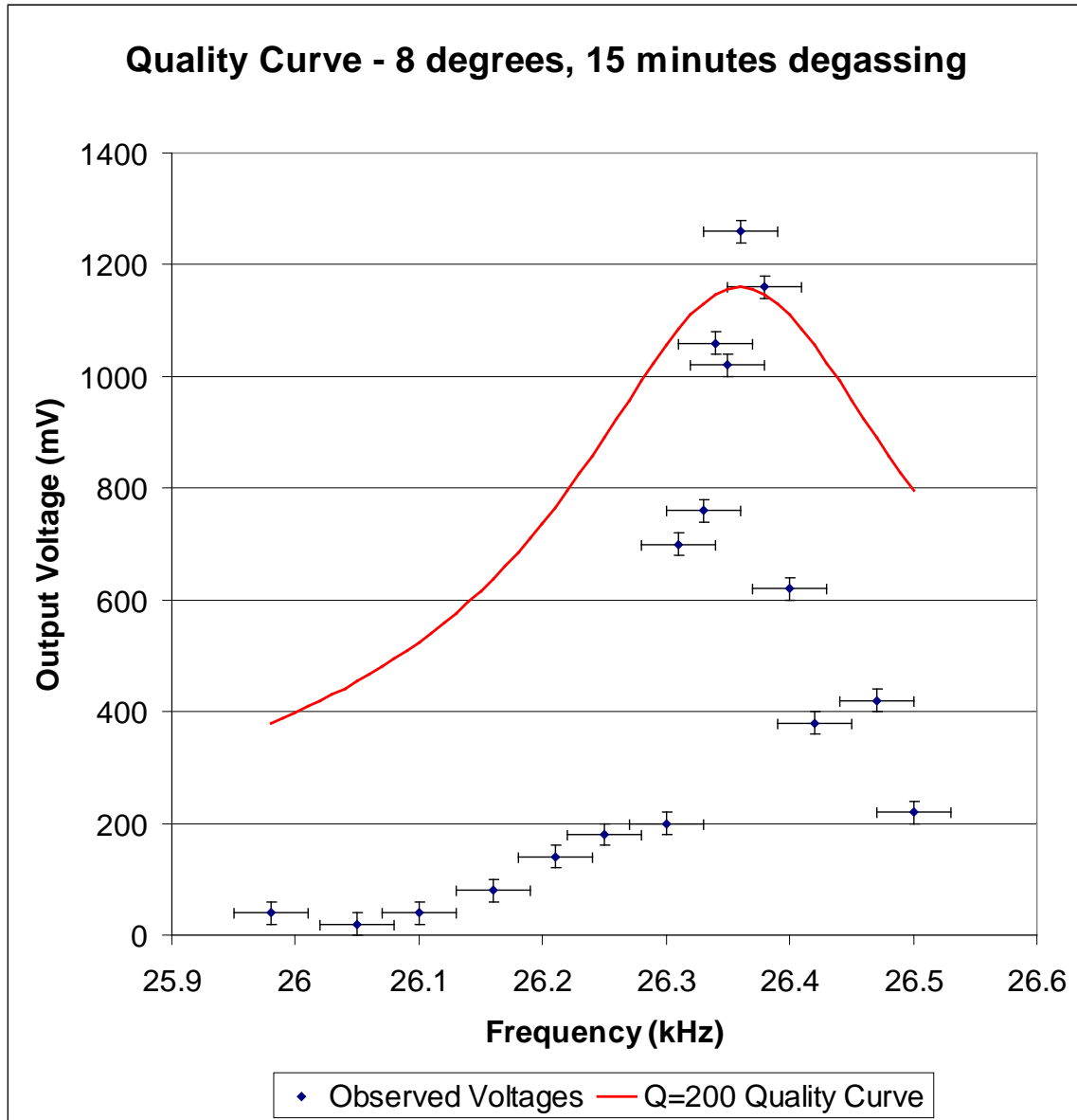
Figure 6: Quality Curve for 7 degree distilled water after 5 minutes degassing.
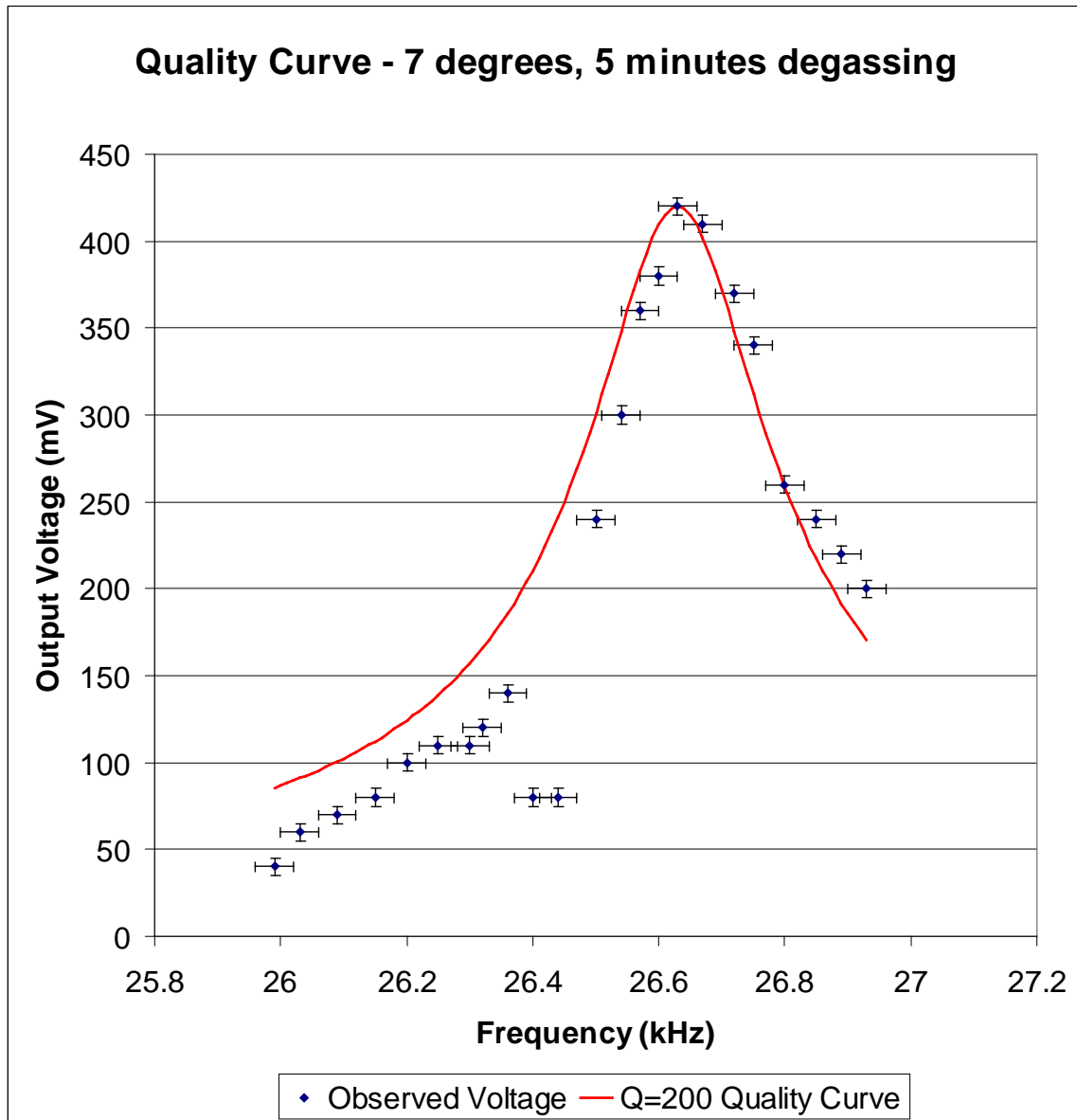
Figure 7: Quality Curve for 9 degree distilled water after 7 minutes degassing.
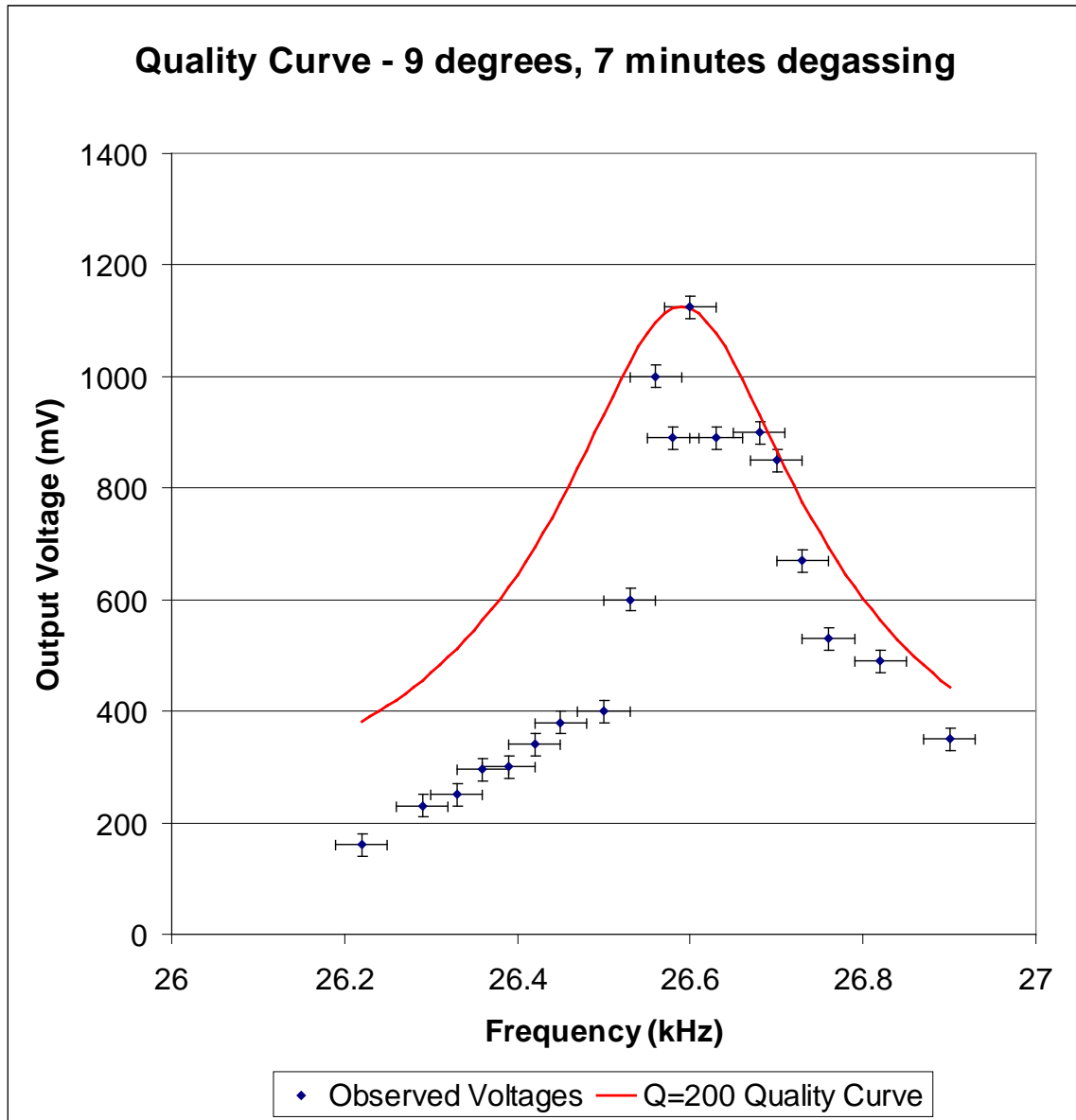
Figure 8: Quality Curve for 9 degree distilled water after 8 minutes degassing.
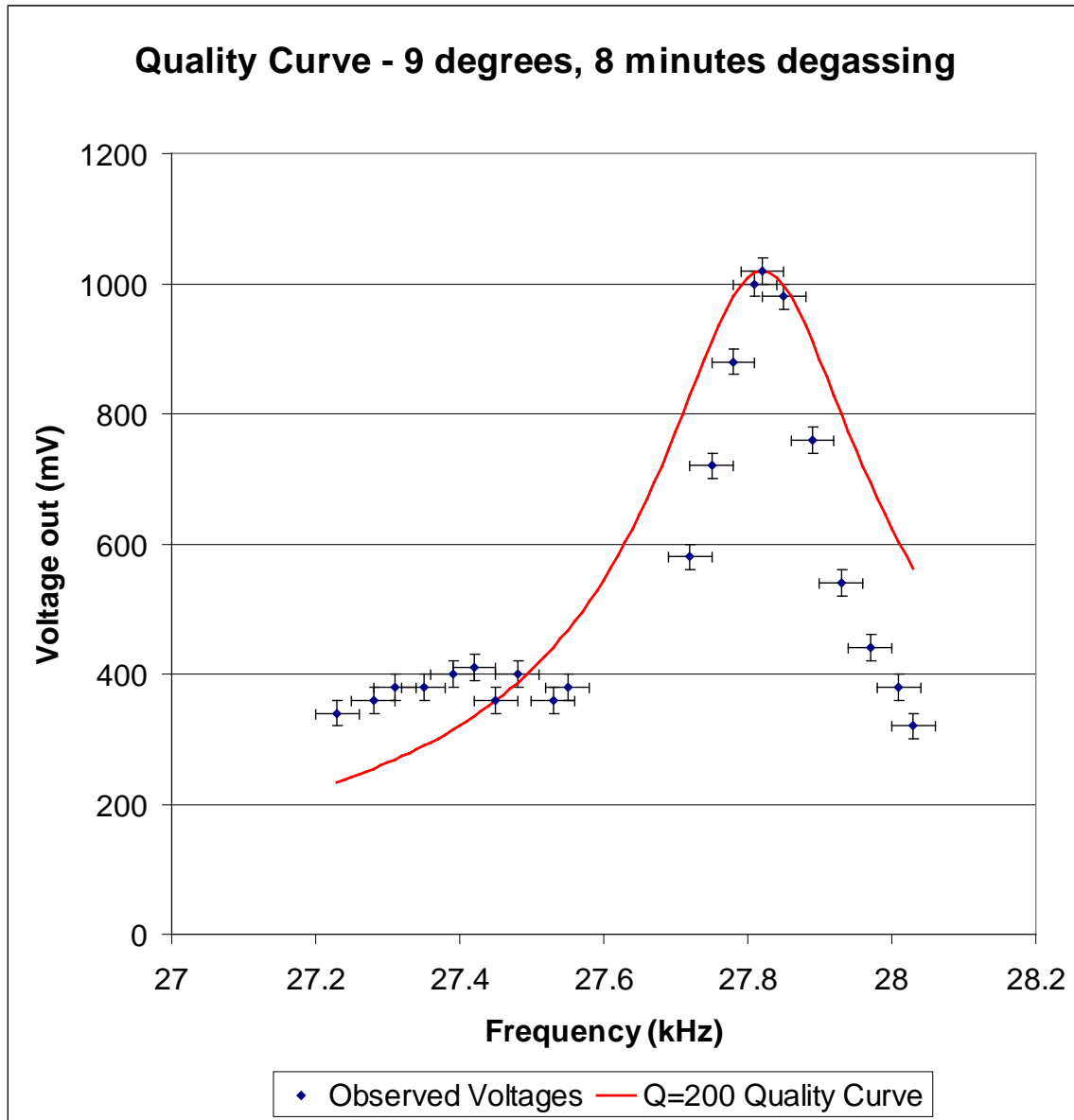
Depending on the preparation of the water in the cell, cavitation bubbles were formed on the immersed surface of the ultrasound horn. These bubbles were pushed from the surface of the horn, and accumulated at the nodes within the cell. As these larger cavitation bubbles disrupted any small trapped bubbles, it was necessary to study this phenomenon in an attempt to reduce it. The number of bubbles on the surface of the horn with respect to temperature is shown in figure 9 below, for 4 different water samples. Each of these samples was distilled water, cooled to the same temperature, however the time spent under vacuum to degas the water differed as noted in the legend.

Figure 9: Cavitation bubble formation versus temperature for 4 water samples.
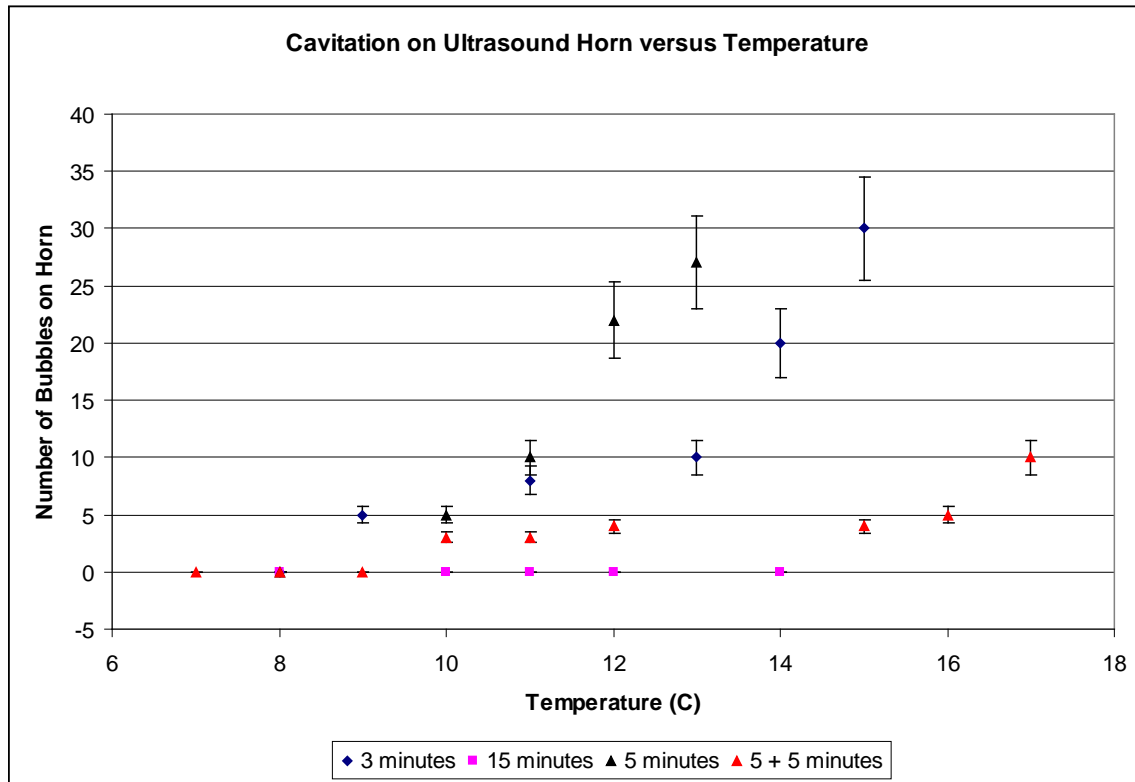
Note in the above figure, that the sample marked 5 + 5 minutes was degassed for 5 minutes, then left to rest in an ice bath for 45 minutes, then degassed for a further 5 minutes. As well, it is clear from the figure that there is a substantial correlation between the concentration of dissolved gasses in the water, and the number of cavitation bubbles formed.

The bubbles formed, either by cavitation, or by boiling, varied in size and stability. The most stable bubbles remained visible within the cell for periods as long as 15 minutes, while the least stable lasted only a few seconds. Again, there is a relation between the concentration of dissolved gasses and the longevity of the bubble, as can be seen in figure 10 below.

Figure 10: Longevity of bubbles with respect to temperature for 4 water samples.
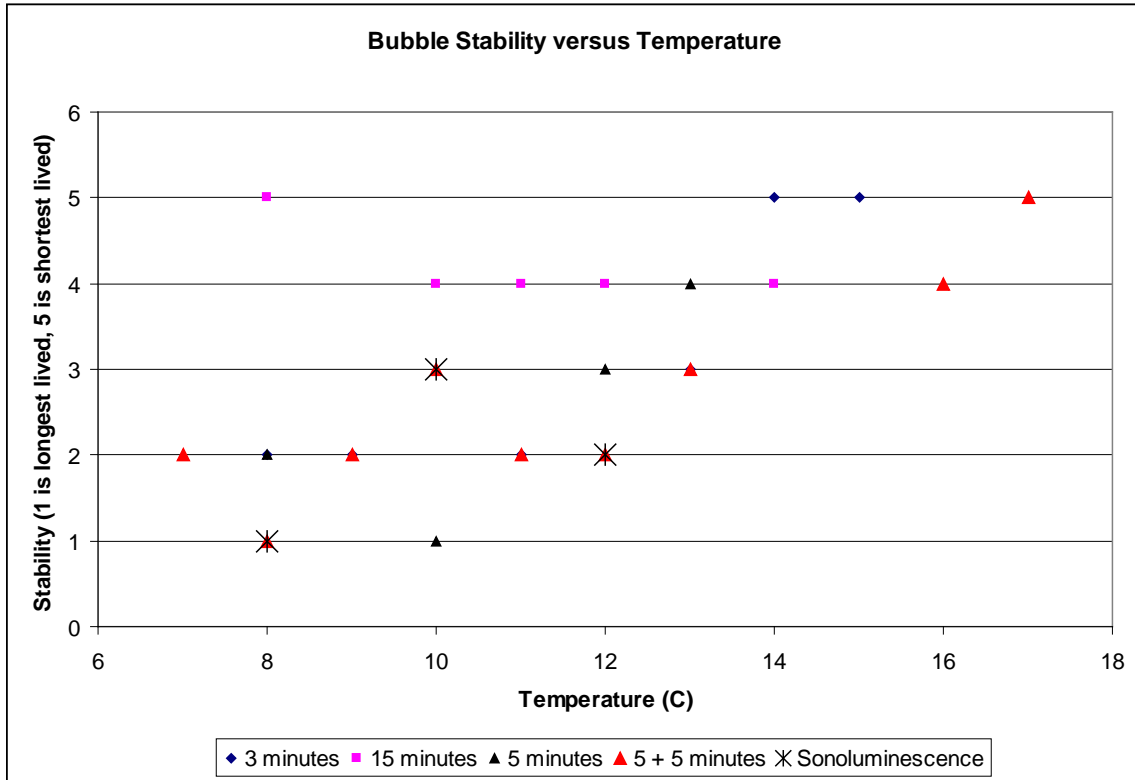
As well, a relation can be seen between the concentration of dissolved gasses and the size of the bubble in figure 11 below.

Figure 11: Trapped bubble size versus temperature for 4 water samples.

Bubble Size versus Temperature
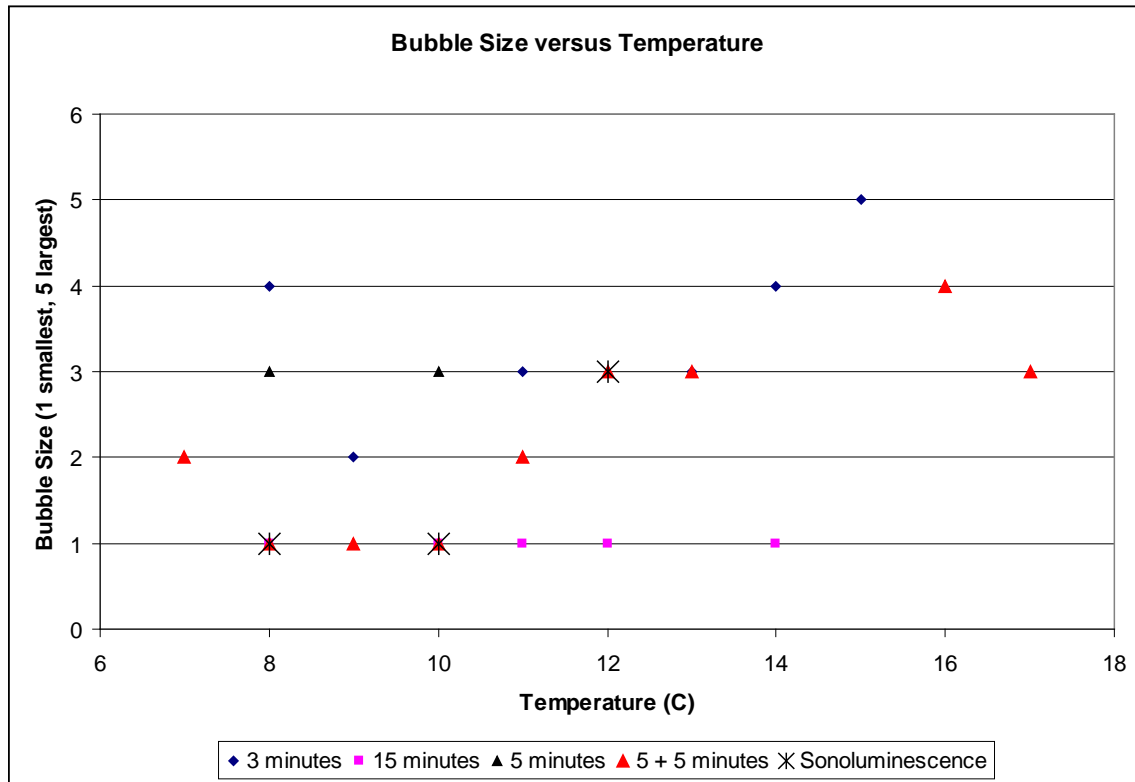
While determining the ideal water preparation technique to use, sonoluminescence was observed. This occurred on the 5 + 5 minute run, as well as on several subsequent runs. In figures 10 and 11, the conditions where sonoluminescence occurred are marked with a star, as shown in the legend.

Subsequent sonoluminescence events were captured using a 15.1 megapixel digital camera, set to a 30 second exposure, film speed ISO 3200. In the images captured, the process of formation of a single sonoluminescent bubble can be seen. Figure 12 shows luminescent bubbles streaming from the filament in the cell, at this point the filament is off.

Figure 12: Multiple Bubble Sonoluminescence near the filament at the bottom of the cell.

Figure 13 shows the bubbles travelling from the filament to the bottom node of the cell. At this point only a faint glow was visible to the unaided eye, this glow is more visible due to the long exposure used here.

Figure 13: Multiple Bubble Sonoluminescence between the filament and the bottom node.
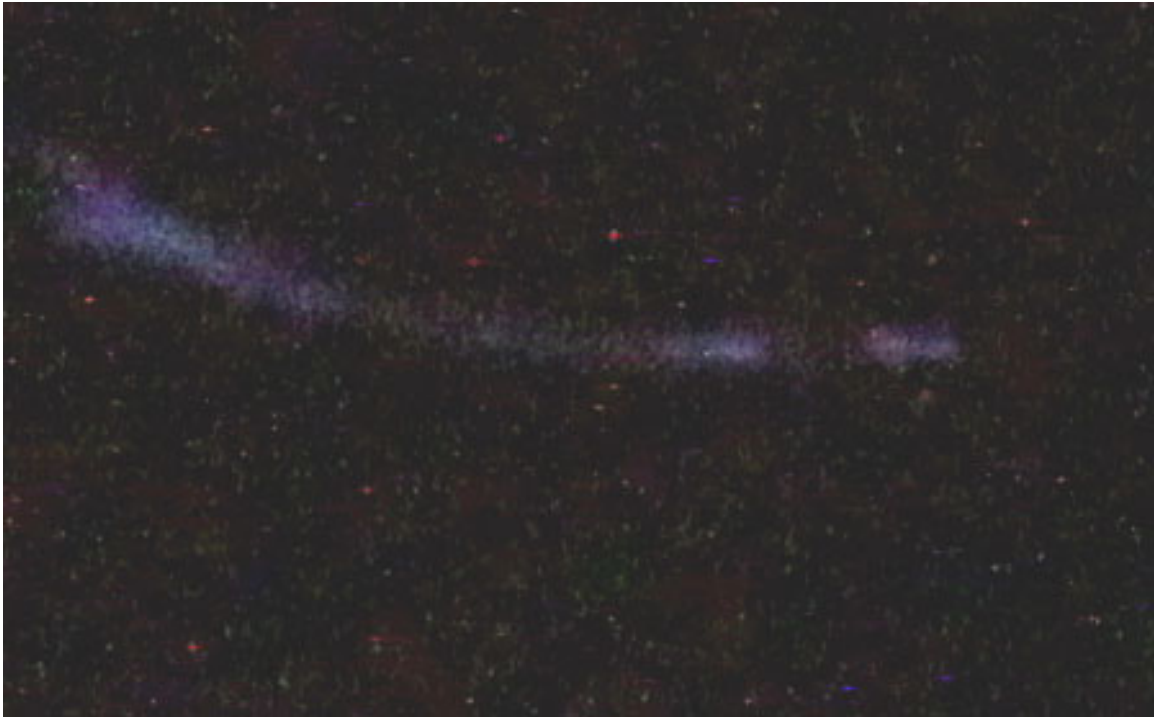
Figures 14, 15, and 16 shows the formation of a single bubble, trapped at the bottom node of the cell. Note as well that the stream of bubbles leaving the filament can still be seen as a tail, to the left of the central bubble.

Figure 14: Single Bubble Sonoluminescence at the bottom node of the cell.

Figure 15: Single Bubble Sonoluminescence at the bottom node of the cell.

Figure 16: Single Bubble Sonoluminescence at the top and bottom nodes of the cell.

Following this, the positions of the nodes within the cell were verified using the hydrophone, the minima and maxima found are listed in table 1 below. Note that all nodes found were located along the centerline of the cell. Additionally, it was not possible to find the location of the topmost minimum, as the horn blocked the hydrophone.

Table 1: Positions of nodes within the resonant cell, distances from bottom of cell.

Maxima	Minima
Distance from bottom of cell (cm)	**Distance from bottom of cell (cm)**
1.65	*0.01*
5.20	*3.50*
8.60	*6.90*

As expected, there were three pressure nodes, found approximately equidistant along the centerline of the cell.

Discussion:

The most straightforward conclusion that can be drawn from this experiment is that water condition is critical for sonoluminescence. The gas content of the water has a significant effect on the size of the bubbles formed, the longevity of the bubbles, as well as the number of cavitation bubbles formed by the ultrasound waves. Complicating this further is the unknown initial conditions of the distilled water. As the solubility of gases in water depends significantly on the temperature, the concentration of those dissolved gases will depend on the temperatures that the water has been stored at, as well as the length of time at those temperatures.

As can be seen in figures 9 and 10, it is clear that there is a middle ground that must be reached as far as gas content is concerned. In the case when the water was degassed for 15 minutes, there were no cavitation bubbles formed at all, however the bubbles were very short lived when generated using the filament. This is expected because the bubbles made using the filament form by boiling the water. If there are no dissolved gases to take the place of the water vapour within the bubble, the vapour will cool and condense, and the bubble will disappear. However in the case when the water was degassed for only 3 minutes, too many cavitation bubbles were formed at the horn, and the motion of these additional bubbles disrupted any trapped bubbles located at the nodes.

As well, a strong relation was observed between signal noise and temperature of the water. The last run conducted, using water that had been degassed for 7 minutes had a clean signal and bright sonoluminescence when the run was started at 8 degrees. Again at 10 degrees, sonoluminescence was observed. However, when the temperature reached 16 degrees Celsius, it was no longer possible to get a clean signal; there was too much noise present. The two signals are shown in figure 17 below, taken from the same water sample at two different temperatures.

Figure 17: Resonance cell output for the same water sample at 8 degrees on the left and 16 degrees on the right.
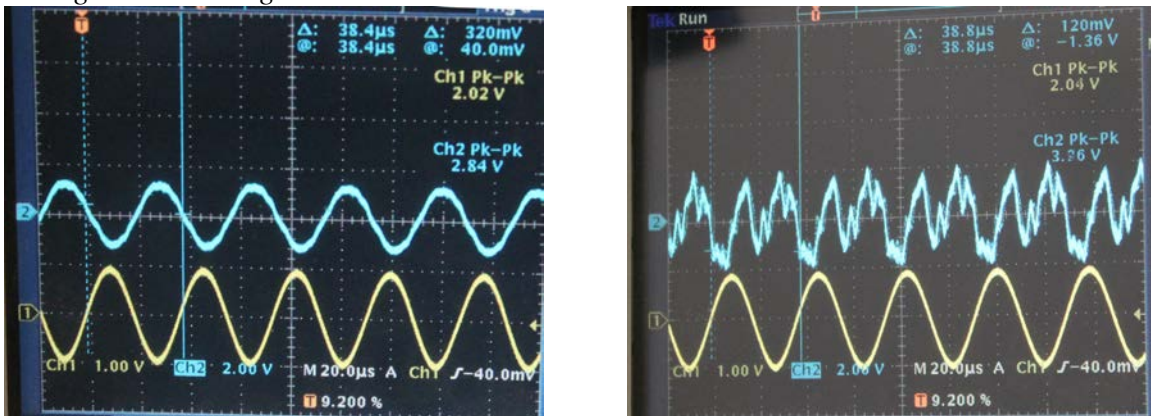
As the noise increased in the output from the cell, so did the motion of the captured bubbles. With a clean sine wave the trapped bubbles remained almost stationary at the pressure nodes within the cell. As noise increased, the bubbles began to jitter from the stationary positions. This jitter may indicate that the bubbles are subject to asymmetric forces as a result of the noise. With the stationary bubbles, the compression forces are acting symmetrically, as there is no net force moving the bubble, other than the force causing the collapse. With the moving bubbles, some unbalanced force must be acting on them to cause that motion.

No sonoluminescence was observed with a noisy signal, thus no sonoluminescence was observed with asymmetrical forces applied to the bubble. Both the shockwave and microjet collapse models allow for sonoluminescence with symmetrical collapse of the bubble. However, only the microjet model would allow sonoluminescence with an asymmetrically collapsing bubble. This is not conclusive evidence supporting the shockwave collapse model over the microjet model, but it does indicate that sonoluminescence is more likely with a symmetrically collapsing bubble.

References:

1. Sonoluminescence: Sound into Light – Putterman 1995 - http://www.physics.carleton.ca/~matanska/PHYS%204008%20lab/Sonoluminescence/Putterman%201995%20reference4.pdf
2. Extracting Light From Water: Sonoluminescence – Guttenkunst 2002 - http://www.physics.carleton.ca/~matanska/PHYS%204008%20lab/Sonoluminescence/Gutenkunst%202002%20reference.pdf
3. Water – Speed of Sound.- http://www.engineeringtoolbox.com/sound-speed-water-d_598.html
4. Universal Resonance Curve - http://www.art-sci.udel.edu/ghw/phys245/05S/classpages/resonance-linear.html
5. European Space Agency: Team Flash and Splash - http://www.flashandsplash.ch/Project/negative.JPG